Characterization and Modeling of Intermodulation Distortion Asymmetry in HBT Using Large-Signal Model

Hyun-Min Park and Songcheol Hong

Dept. EECS, Korea Advanced Institute of Science and Technology (KAIST)
373-1, Guseong-dong, Yuseong-gu, Daejeon, 305-701, Republic of Korea

Abstract — **Asymmetrical behaviors of intermodulation distortion (IMD) in microwave active devices are often observed when the terminating impedance at baseband frequency contains a reactive component. This phenomenon sometimes induces misunderstanding of distortion performance unless the baseband impedance effects are properly accounted for. The distortion asymmetry appears in not only small-signal regime but also large-signal regime. Therefore, a unified approach which can predict IMD asymmetry over a broad range of output power levels is in critical demand. In this context, the usefulness of nonlinear large-signal model is addressed when predicting IMD asymmetries. Extensive measurement results are compared to simulation results to demonstrate the usefulness. Moreover, the origin of distortion asymmetry is discussed with time-domain envelope simulation.**

I. Introduction

The most frequently used linearity figure-of-merit of nonlinear microwave circuit is the ratio of the inband signal power relative to the out-of-band distortion signal power. This ratio is known as the carrier to intermodulation distortion (IMD) ratio when two equal signals with slightly different frequencies are applied. The difference of applied frequency, which is termed as baseband (or envelope) frequency, influences the observed IMD in a complicated way and sometimes leads to an imbalance between the upper and lower IMDs under certain circumstances. As a result, the relative signal strength of the upper IMD differs from that of the lower IMD. Moreover, the absolute strength also changes with the envelope frequency due to the secondary order effects often caused by self-heating of active devices. Therefore, it is necessary to understand these anomalous behaviors for a successful circuit design. Moreover, it is advantageous to be equipped with a tool which can accurately predict these phenomena accurately. In power amplifier circuit, the device usually experiences the extreme operating dynamics ranging from pinchoff to saturation. In this case, the analytical approach, such as Volterra series [1]-[4], fails to achieve an accurate predictability.

In this paper, the versatility of large-signal model in prediction of incalculable IMD is addressed. Extensive measurement results will be compared to the simulation results to demonstrate the benefit of the method. At first, the measurement results of various HBTs as a function of envelope frequency as well as bias current level will be given to reveal the general trend of IMD asymmetry. After that, self-heating effect on IMD behavior will be discussed based on whether this effect is taken into account in the model or not. Finally the physical origin of the asymmetry will be addressed by analyzing harmonic balance simulation result obtained from large-signal model.

II. Measurement

The conventional two-tone setup was configured under on-wafer environment to obtain measurement data. The fundamental and higher harmonic impedances are set to 50 Ω to facilitate the matching task. The baseband impedance is determined by the bias network which is composed of a bias tee and a DC feeding cable. This network provides nearly short impedance at low envelope frequency. However, it gradually becomes open-circuited at higher frequency due to the RF choke of bias tee. The device will therefore see 50 Ω at RF frequencies. During the transition, the rapid sign reversal of reactive component of baseband impedance can occur at several resonance points. This situation was adopted in this study since it could be a realistic representation of a practical situation in high frequency circuit. The baseband impedance of the measurement setup was measured from 0.1 to 100 MHz and is displayed in Fig. 1.

To observe the asymmetrical behavior in IMD, 1, 2, and 6finger InGaP/GaAs HBTs with a unit emitter area of 2x30 μm^2 were measured under the same setup. The bias current for each device were set to 3, 5, and 7 mA respectively to ensure class AB operation. The collector bias was set to 3.5 V for all devices. Input power level was carefully adjusted such that the output power from all three devices was similar (Pout = 0 dBm).

Fig. 2 shows the measured IMD3 difference (IMD3D) as a function of two-tone spacing frequency at a center frequency of 500 MHz. It can be easily seen that IMD3D follows the transitional pattern of the imaginary part in baseband impedance. Each device shows a similar trend with tone spacing frequency. Thus, it is clear that the baseband impedance is a major source for IMD asymmetry.

III. Large-Signal Model

To characterize the IMD asymmetry, large-signal models

0-7803-7695-1/03/$17.00 © 2003 IEEE

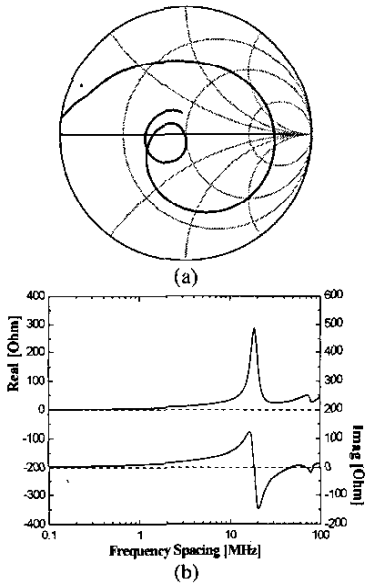

Fig. 1. The measured impedance of input network: (a) reflection coefficient, and (b) real and imaginary part.

for the devices were extracted based on the approach in [5]. This model is very effective in prediction of thermal effects in HBT. The model is a modified Gummel-Poon topology with feedback elements to describe the temperature effect of HBT. A unified approach is adopted in this model to incorporate the ambient temperature and self-heating effects simultaneously. The extraction procedure is described in detail in the literature.

After incorporating the measured baseband impedance into the simulator, harmonic balance simulations were performed at the same bias condition by using the extracted large-signal model. Fig. 3 shows the comparison between the simulated and measured IMD asymmetry for 6finger device. The correlation is very good, which ascertains the advantage of large-signal model. The same degree of correlation was achieved for the other devices.

When measuring IMD asymmetry, it was also found that the absolute signal strengths of the upper and lower IMDs were dependent on the envelope frequency. They gradually improved with the envelope frequency, but suddenly peaked at 20 MHz where the magnitude of baseband impedance showed a maximum value. To investigate these phenomena, two distinct cases were simulated and displayed in Fig. 4:

Case A – Thermal time constant (τ_{th}) is infinite. Therefore, temperature variation is not modeled during envelope signal swing. Device junction temperature is set constant to a value determined by the applied bias.

Case B – τ_{th} is finite. The temperature increase is felt at low envelope frequency. The exact value can be set by thermal capacitance (C_{th}).

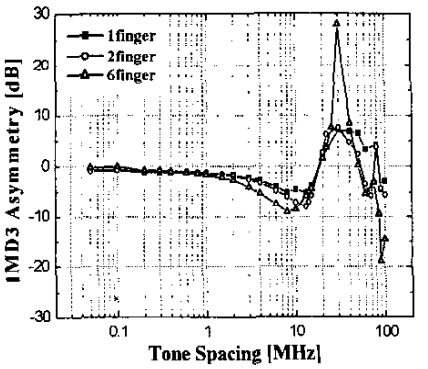

Fig. 2. Measured IMD3 asymmetry as a function of tone spacing at fc = 0.5 GHz and V_{CE} = 3.5 V.

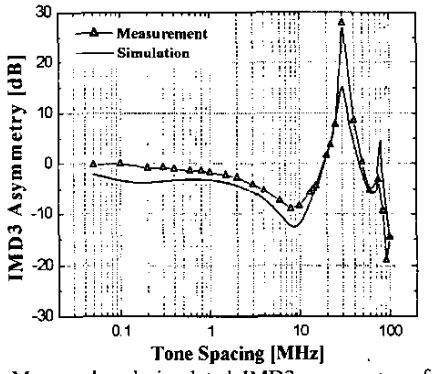

Fig. 3. Measured and simulated IMD3 asymmetry of 6finger device at fc = 0.5 GHz and V_{CE} = 3.5 V.

When the device is biased for class AB operation, the bias modulation effect [6] further distorts the RF signal envelope hence results in reduced signal purity. Therefore, IMD degradation can be seen in case B at low envelope frequency range. The modulation effect disappears at high envelope frequency even in case B since the upper frequency was set by τ_{th}. The junction temperature in this case remains constant during envelope signal swing. As a result, case B produces the similar results as case A at these regions. It is concluded that the self-heating effect degrades IMD and promotes the asymmetry further especially in low envelope frequency. It is also noted that the simulation with thermal effect being included is more accurate in prediction of distortion behavior.

The IMD can change considerably in accordance with the applied bias current. Several mechanisms were identified in HBT, where the nonlinearities from different elements cancel each other. There is a sudden improvement in IMD when this cancellation occurs, which is known as a sweet spot. The IMDs are more susceptible to magnitude imbalance due to their weak strengths in a sweet spot [7].

To study IMD asymmetry in sweet spot, the devices were measured as a function of bias current with the tone spacing frequency being fixed at 2 MHz. Fig. 5 shows the comparison results for all devices. Each device showed a distinct bias current level for enhanced IMD asymmetry.

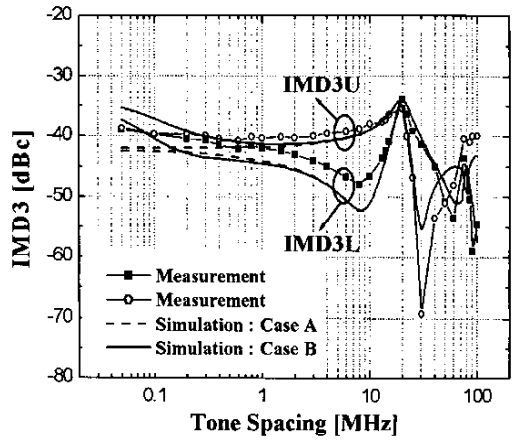

Fig. 4. Measured and simulated lower and upper IMDs of 6finger device at fc = 0.5 GHz, V_{CE} = 3.5 V, and I_C = 7 mA.

When the upper and lower IMDs of 1finger device are plotted as in Fig. 6, they indeed improve around a sweet spot. It is advantageous to bias the device at sweet spot to exploit the enhanced linearity. But one should be cautioned not to misjudge linearity figure-of-merit since considerable asymmetry can occur even at relatively small tone spacing frequency. The simulation result tracks measurement data well. This means that the large-signal model is very effective in predicting bias condition for sweet spot and the amount of IMD asymmetry.

The linearity performance at various output levels is another frequently used characterization method of an active device. Fig. 7 illustrates the two-tone results of 6finger device under power sweep condition at 10 and 30 MHz, respectively. At 10 MHz, the baseband impedance is characterized by a positive reactance while at 30 MHz it is characterized by a negative reactance. As a result, the dominance between the upper and lower IMDs changes with the change of tone spacing frequency. Although these characteristics can be predicted by large-signal model readily, they are not easily expressed in an analytical equation by Volterra series method whose validity is limited to weakly nonlinear regime. The advantage of large-signal model is evident in this sort of characterization.

IV. Discussion

To investigate the origin of IMD asymmetry, load line simulations at envelope frequency were performed at 10 and 30 MHz tone spacing frequency as shown in Fig. 8. The output power was set to 17 dBm which amounts to 1 dB backoff from P_{1dB}.

When Δf = 10 MHz, the situation can be described as follows: The baseband impedance is characterized by a positive reactive component. This means that the voltage source with inductive output impedance is connected to the collector of DUT. The voltage source supplies envelope

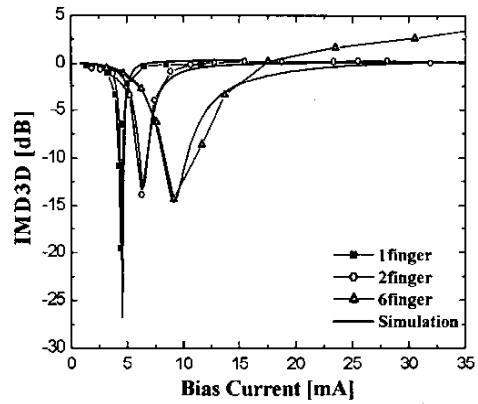

Fig. 5. Measured and simulated IMD3 asymmetry as a function of bias current at fc = 0.5 GHz, V_{CE} = 3.5 V, and Δf = 2 MHz (symbol–measurement, line–simulation).

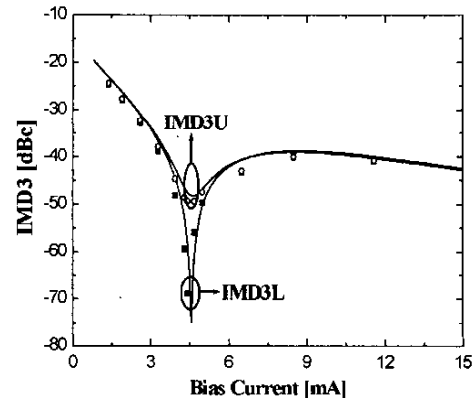

Fig. 6. Measured and simulated lower and upper IMD3 of 1finger device as a function of bias current at fc = 0.5 GHz, V_{CE} = 3.5 V, and Δf = 2 MHz (symbol–measurement, line–simulation).

current to DUT. When the DUT is biased at class AB operation, the output signal distortion occurs during envelope swing due to the pinchoff and saturation. In Fig. 9(a), there is a region where the output voltage increases while the current remains at a very small value at pinchoff region. Since the inductive source tends to resist the abrupt increase of its outgoing current, the load line is formed in a way that it loops clockwise in the upper oval as shown in Fig. 8(a). Therefore, the current and voltage waveforms are asymmetrical on either side of π axis as depicted in Fig. 9(a).

However, the capacitive source at Δf = 30 MHz tends to block the abrupt change of its incremental voltage, the load line in this case loops counterclockwise in the upper oval as shown in Fig. 8(b). The resultant envelope in Fig. 9(b) resembles the mirror image of the previous case along π axis. Therefore, the dominance between the upper and lower IMDs is determined by the envelope signal distortions from these two distinct mechanisms.

V. Conclusion

The IMD simulations under various conditions have been performed using nonlinear large-signal model. It is found that the absolute signal strengths as well as the asymmetry of IMD can be predicted well by this approach. The envelope simulation, which is feasible due to the large-signal model, revealed the physical mechanisms for IMD asymmetry. It is also concluded that an accurate modeling of self-heating effect is very important in prediction of IMD behavior in low envelope frequency range.

Acknowledgement

This work was supported by KOSEF under the ERC program through the MINT research center at Dongguk University.

References

[1] Bo Wang, Xingnan Hong, and Baoxin Gao, "A new method to find the optimal subharmonic impedance for CDMA power amplifier with Volterra series analysis," in *Proceedings of 2001 Asia-Pacific Microwave Conference*, 2001, pp. 306-309.

[2] Joel Vuolevi, Timo Rahkonen, and Jani Manninen, "Measurement technique for increasing the linearity by optimising the source impedance of RF power amplifiers," in *IEEE Radio and Wireless Conf.*, 2000, pp. 227-230.

[3] Vladimir Aparin and Charles Persico, "Effect of out-of-band terminations on intermodulation distortion in common-emitter circuits," in *IEEE MTT-S Int. Microwave Symp. Dig.*, 1999, pp. 977-980.

[4] John F. Sevic, Kerry L. Burger, and Michael B. Steer, "A novel envelope-termination load-pull method for ACPR optimization of RF/Microwave power amplifiers," in *IEEE MTT-S Int. Microwave Symp. Dig.*, 1998, pp. 723-726.

[5] Hyun-Min Park, Ron Green, and Songcheol Hong, "A novel extraction method for a fully electro-thermal large-signal model of HBT," in *IEEE MTT-S Int. Microwave Symp. Dig.*, 2002, pp. 1009-1012.

[6] Ke Lu, Paul M. McIntosh, Christopher M. Snowden, and Roger D. Pollard, "Low-frequency dispersion and its influence on the intermodulation performance of AlGaAs/GaAs HBTs," in *IEEE MTT-S Int. Microwave Symp. Dig.*, 1996, pp. 1373-1376.

[7] Nuno B. Carvalho and Jose C. Pedro, "Two-tone IMD asymmetry in microwave power amplifiers," in *IEEE MTT-S Int. Microwave Symp. Dig.*, 2000, pp. 445-448.

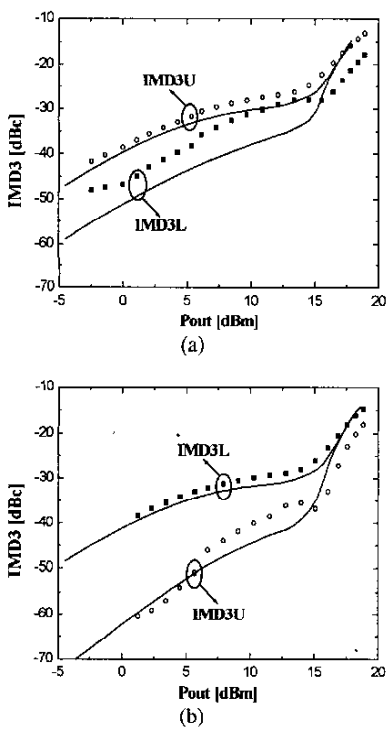

Fig. 7. Measured and simulated lower and upper IMD3 as a function of output power at fc = 0.5 GHz, V_{CE} = 3.5 V, and I_C = 7 mA (symbol–measurement, line–simulation). (a) Δf = 10 MHz and (b) Δf = 30 MHz.

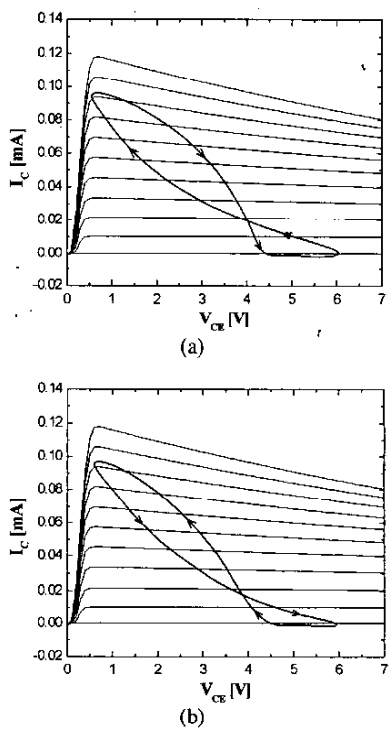

Fig. 8. Load line simulation results of 6finger device at fc = 0.5 GHz, V_{CE} = 3.5 V, and I_C = 7 mA. (a) Δf = 10 MHz and (b) Δf = 30 MHz.

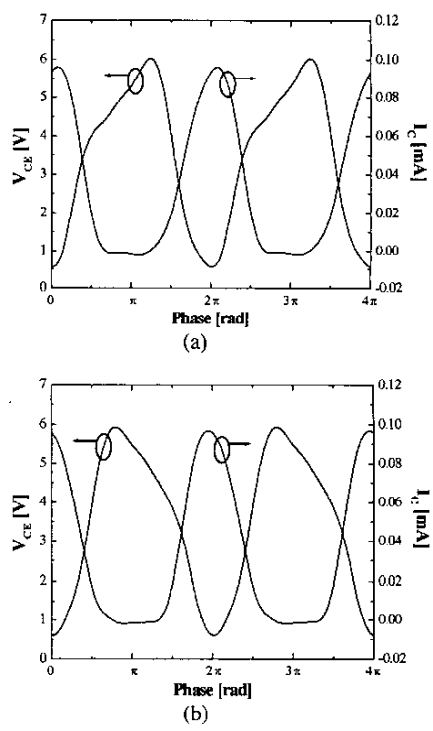

Fig. 9. Simulated current and voltage waveforms of 6finger device at fc = 0.5 GHz, V_{CE} = 3.5 V, and I_C = 7 mA. (a) Δf = 10 MHz and (b) Δf = 30 MHz.